

CONSTRUCTION OF A MECHANISM OF PHYSICOCHEMICAL PROCESSES BEHIND A SHOCK WAVE PROPAGATING IN THE ATMOSPHERES OF PLANETS

V. N. Makarov

UDC 533.6.01+533.72+519.6

The problems of construction of a kinetic model of a medium (gas, plasma) based on the choice of the most important physicochemical processes are considered. The optimum kinetic mechanisms of a medium that describe the main nonequilibrium processes behind the shock-wave front are constructed with the example of the problem of propagation of a direct shock wave in the atmosphere of planets of the solar system. The investigations have been carried out using an automated system described earlier.

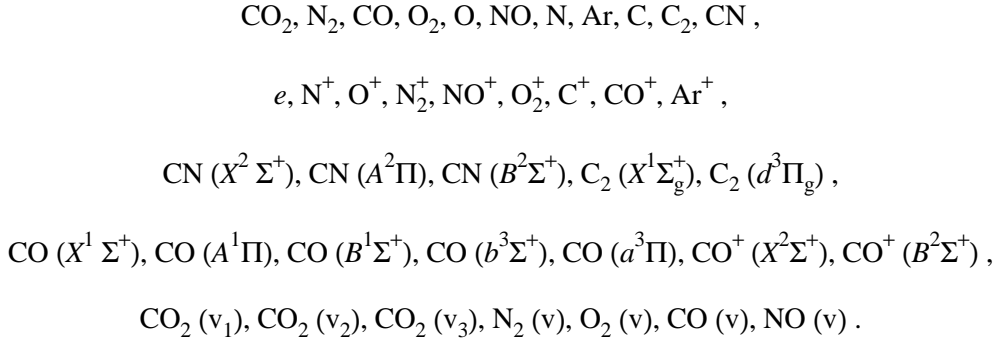
In connection with the expected flights to the planets of the solar system (Venus, Mars), there appeared numerous works devoted to nonequilibrium physicochemical processes in the atmospheres of these planets [3–8]. In a number of these works, the radiation from atmospheric gases was assumed to be locally equilibrium. However, even in early investigations (carried out in both air and a CO₂–N₂ mixture), it was established that behind a shock wave the Boltzmann distribution of particles over electronically excited states can be disrupted [7, 8]. This leads to a significant difference between the detected values of the radiation intensity and its locally equilibrium values. Thus, in the calculations of the radiation from atmospheric gases one must consider additionally the possibility for the electronically excited states of molecules to form directly as a result of chemical transformations. When the velocities of entry into the atmosphere are high, the radiation from the CO₂–N₂ mixtures can contribute substantially to the total heat flux toward the surface of a descent module of a spacecraft. However, even in the case where the entry velocity is low and this radiation has no influence on the heat exchange, it remains an important characteristic determining the operation of optical devices aboard the descent module [6].

In the present work, we constructed optimum kinetic mechanisms of the main physicochemical processes in a gas behind a shock wave that describe the radiation-intensity distribution, the electron concentration, and the translational temperature of the gas.

Kinetic Model of High-Temperature Radiating CO₂–N₂–Ar Mixtures. The calculational investigations were carried out using an automated system [1, 2] in which the following units are functioning and interacting: structurized bases of kinetic data; a generator of kinetic equations that allows one, using the data bases, to efficiently form the functional relations describing changes in nonequilibrium variables; a software system for direct calculation allowing the modeling of the flow field (with regard for the nonequilibrium processes); a programmed module for construction of a kinetic mechanism of the most important processes occurring in a gas medium; a programmed module for a search for the optimum conditions of functioning of the investigated object.

In the numerical modeling of nonequilibrium processes occurring in a gas CO₂ + N₂ + Ar mixture at high temperatures, we took into account the following chemically active particles and their electronic and vibrational states:

Institute of Mechanics, M. V. Lomonosov Moscow State University, Moscow, Russia: email: vmakarov@inmech.msu.su. Translated from *Inzhenerno-Fizicheskii Zhurnal*, Vol. 74, No. 2, pp. 87–92, March–April, 2001. Original article submitted March 28, 2000.



In the last line, the symbol v denotes a vibrationally excited molecule (symbols v_1 , v_2 , and v_3 denote, respectively, the symmetric, deformation, and antisymmetric types of vibrations of CO_2 molecules).

In such modeling of the processes in shock waves propagating in the atmosphere of Mars (or Venus), the electronic states of molecules excited with the participation of N particles (besides CN) were not taken into account, since the initial concentration of N_2 molecules is much lower than the concentration of CO_2 molecules (the modeled composition of the Mars atmosphere was as follows: 96% of CO_2 + 3% of N_2 + 1% of Ar).

The base of kinetic data that was used for modeling of relaxation processes behind a shock wave in the Mars atmosphere at high temperatures contained information on the following processes: chemical reactions with the participation of neutral and charged particles, processes of excitation and deactivation of electronic states of molecules, radiation processes with the participation of electronically excited particles, processes of vibrational–translational (VT) and vibrational–vibrational (VV') energy exchange with the participation of different modes of multiatomic molecules, and CV processes involving chemical reactions that determine the vibrational relaxation [2, 6]. The rate constants of the main chemical and ionization reactions have been taken from the literature data [3–6, 9], and a certain part of the excitation cross sections of the electronic states of CN and C_2 molecules that are the main sources of radiation was determined earlier from the appropriately processed data of special experiments carried out in a shock tube [6]. The values of the inverse rate constants of the reactions proceeding with the participation of neutral and charged particles were calculated in terms of the equilibrium constant with the use of a reduced thermodynamic potential [10]. The times of the vibrational energy exchange are indicated in [6].

In a nonequilibrium gas where an equilibrium between the translational and vibrational degrees of freedom of molecules-reagents is absent, the rate constant of a chemical reaction depends not only on the translational temperature T but also on the vibrational temperature T_v . In this case, the rate constant is conveniently written in the form $k(T, T_v) = Z(T, T_v)k^0(T)$, where $k^0(T)$ is a thermally equilibrium rate constant and $Z(T, T_v)$ is the nonequilibrium factor. An analysis of the available two-temperature models of the rate constants of chemical reactions and of the nonequilibrium factor is given in [11]. We used the Kuznetsov model [12] to describe the thermally nonequilibrium decay of CO_2 molecules.

In collisional processes that lead to the excitation of electronic states, electrons are very active. The electron temperature T_e in the gas behind the shock-wave front was determined using the equation of electron-energy balance $n_e \sum_k Q_k^e = 0$, where Q_k^e is the rate of energy exchange between the electrons for different processes (elastic collisions with atoms and molecules; elastic collisions with ions; excitation of molecule rotations; excitation of molecular vibrations; excitation of electronic states of atoms and molecules; ionization of atoms, molecules, and recombination of charges) [6].

Construction of a Kinetic Mechanism of the Main Processes. One of the primary goals of the modeling of kinetic processes in gas dynamics is the development of minimum-complexity mechanisms that would allow one to describe adequately the basic phenomena in gases and the experimental data obtained. In

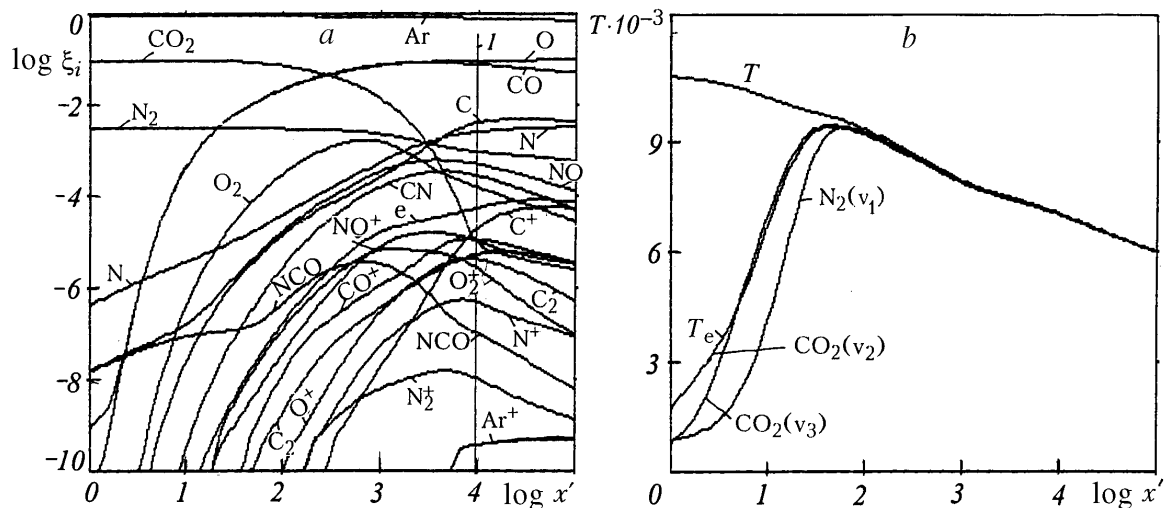


Fig. 1. Distributions of the molar fractions ξ_i for neutral and charged particles (a) and of the translational T , electronic T_e , and vibrational temperatures (b) versus $x' = \log (x/L_f)$. $P_1 = 133.3$ Pa, $V = 3.45$ km/sec, 9.6% of $\text{CO}_2 + 0.3\%$ of $\text{N}_2 + 90.1\%$ of Ar.

solution of this problem, it is necessary, as a rule, to answer the following questions: what stages of the analyzed kinetic system determine the kinetics of one component or another (an arbitrary functional in the general case), what stages are redundant for the considered system, and it can be simplified? Thus, solving a concrete problem, a researcher can propose choosing the data on the most important physicochemical processes from the data base.

In [1, 2, 9], the problem of determination of a compact mechanism of the main processes has been formulated and solved relative to arbitrary functionals φ dependent on both the nonequilibrium and gasdynamic variables, and the mechanism obtained satisfies the condition of minimality in the number of elementary stages. In fact, this means that for each value of the threshold accuracy ε there are a minimum number of main processes, the use of which in modeling guarantees the fulfillment of the accuracy criterion

$$|\varphi_0 - \varphi_*| \leq \varepsilon |\varphi_0|, \quad (1)$$

where φ_0 is the value of the investigated functional φ with regard for the initial base of kinetic data and φ_* is the value of φ for the subset of the main kinetic processes. The mechanism of the main processes is optimum if a further procedure of elimination of elementary processes from the data base leads to the violation of inequality (1).

Investigation Results. Using the above-mentioned base of kinetic data, we calculated the concentrations of particles in the ground and excited states behind the front of a shock wave propagating in the Mars atmosphere and in the mixture 10% of the Mars atmosphere + 90% of Ar for shock-wave velocities V to 11 km/sec and pressures on the order of several torr. The calculation data obtained were compared to the analogous data obtained by other authors, in particular, to the data from [3] obtained for the Mars atmosphere. Our results were found to be close to the data from [3] in concentration of neutral and charged particles, vibrational temperature, and equilibrium radiation intensity. We note that in [3], the nonequilibrium distribution of electronically excited particles was not taken into account.

Figure 1a shows the changes in the concentrations of the components of neutral and charged particles behind the shock-wave front. The initial pressure P_1 , the shock-wave velocity V , and the composition correspond to the experimental data from [6]. It is seen from the figure that the changes in the concentrations of the components in the region of experimental measurements are nonequilibrium in character (the duration of

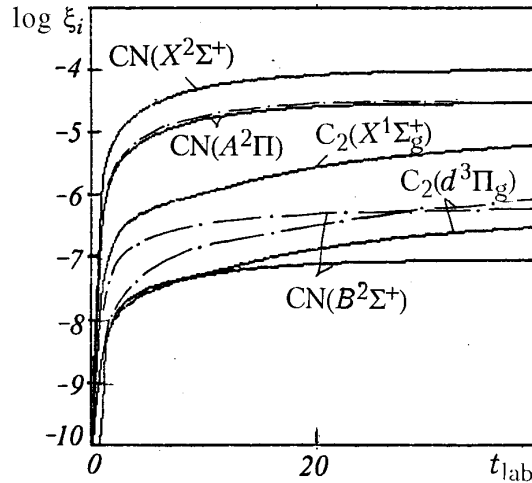


Fig. 2. Distribution of the molar fractions ξ_i of $\text{CN}(X^2\Sigma^+)$, $\text{CN}(A^2\Pi)$, $\text{CN}(B^2\Sigma^+)$, $\text{C}_2(X^1\Sigma_g^+)$, and $\text{C}_2(d^3\Pi_g)$ particles versus laboratory time $t_{\text{lab}}(\mu\text{sec})$ in the region of experimental measurements. $P_1 = 133.3 \text{ Pa}$, $V = 3.45 \text{ km/sec}$, 9.6% of $\text{CO}_2 + 0.3\%$ of $\text{N}_2 + 90.1\%$ of Ar .

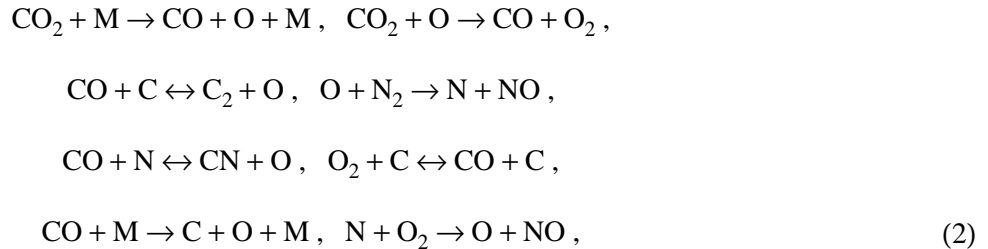
the gas luminescence behind the shock-wave front is denoted by the vertical line 1). In Fig. 1a, the distributions of the concentrations of electronically excited particles that determine the radiation spectrum behind the wave are omitted: the data necessary for this case are given in Fig. 2. Figure 1b shows the analogous distributions of the translational T_1 , electronic T_e , and vibrational temperatures. It is seen that in the region of experimental measurements, all the temperatures are close to each other.

Figure 2 shows the changes in the concentrations of $\text{CN}(A^2\Pi)$, $\text{CN}(B^2\Sigma^+)$, $\text{C}_2(d^3\Pi_g)$, $\text{CN}(X^2\Sigma^+)$, and $\text{C}_2(X^1\Sigma_g^+)$ particles behind the shock-wave front that correspond to the data of experiments carried out in a shock tube [6]. The experimental and calculated radiation distributions obtained for the best chosen rate constants of the excitation and deactivation of the electronic states of $\text{CN}(A^2\Pi)$, $\text{CN}(B^2\Sigma^+)$, and $\text{C}_2(d^3\Pi_g)$ particles are given in [6]. Comparison of these data shows that the agreement between them occurs in the region of violet and red CN bands and in the Swan band for the C_2 molecules. The dash-dot lines in Fig. 2 correspond to the model in which the populations of the electronic states of $\text{CN}(A^3\Pi)$, $\text{CN}(B^2\Sigma^+)$, and $\text{C}_2(d^3\Pi_g)$ particles satisfy the Boltzmann distribution. It follows from the results presented that the population of the states of $\text{CN}(B^2\Sigma^+)$ and $\text{C}_2(d^3\Pi_g)$ differs significantly from the Boltzmann distribution, and the population of the states of $\text{CN}(A^2\Pi)$ is close to the Boltzmann distribution, which finally warrants the use, in modeling, of an approximation in which each of the electronically excited states is considered as an individual component whose concentration is determined from the corresponding kinetic equation.

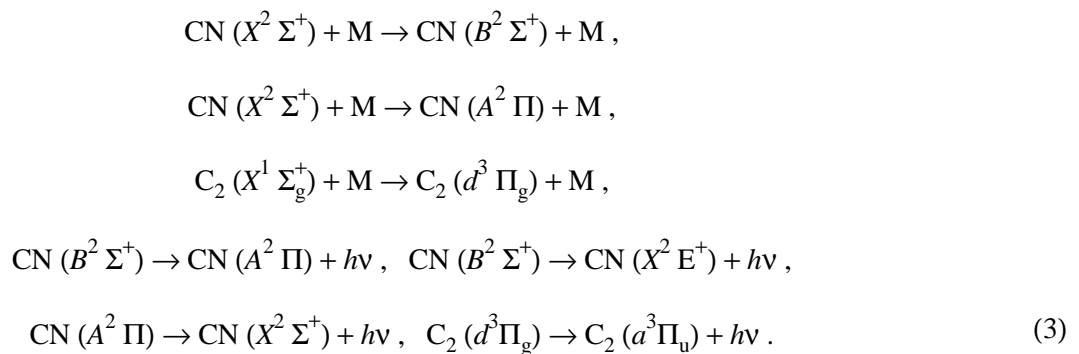
To construct the kinetic mechanism in accordance with criterion (1) determining the concentrations of electronically excited states of $\text{CN}(A^2\Pi)$, $\text{CN}(B^2\Sigma^+)$, and $\text{C}_2(d^3\Pi_g)$, we used the base of kinetic data on 124 chemical reactions. In this case, we used the model of one-temperature kinetics, since, according to the calculation data from [6], the distributions of the concentrations of particles in the Mars atmosphere differ little from each other.

The constructed kinetic mechanism of the main stages can depend substantially on the concrete form of the functional φ , the accuracy ε , and the initial and boundary conditions as far as the nonequilibrium and gasdynamic variables are concerned. In particular, a change in the parameters (in the temperature, first of all) of the gas behind a shock wave can lead to a significant change in the characteristic times of the elementary stages and to a transformation of the kinetics of the main processes. Thus, for the chosen functional φ and the given accuracy ε , the mechanism of the main processes behind a shock wave in the Mars atmosphere will depend on the velocity of its propagation.

If the distribution of the concentrations of $\text{CN}(A^2\Pi)$, $\text{CN}(B^2\Sigma^+)$, and $\text{C}_2(d^3\Pi_g)$ with a threshold accuracy $\varepsilon = 0.3$ is chosen as the investigated functional φ , for the shock-wave-front velocities $5 \text{ km/sec} \leq V \leq 7 \text{ km/sec}$ ($P_1 = 133.3 \text{ Pa} = 1 \text{ torr}$) the mechanism will include the following reactions with the participation of neutral particles:



and also the processes



The problem was solved under the assumption that the length of the considered relaxation zone is equal to 1 m. In order that the criterion (1) be fulfilled for the velocity $V = 8 \text{ km/sec}$, the mechanism (2) should be extended due to the reaction of dissociation of NO molecules, i.e., due to the $\text{NO} + \text{M} \rightarrow \text{N} + \text{O} + \text{M}$ channel, and for the velocity $V = 9 \text{ km/sec}$ it should additionally include the reactions $\text{CN} + \text{O} \leftrightarrow \text{NO} + \text{C}$, $\text{CN} + \text{N} \rightarrow \text{C} + \text{N}_2$, and $\text{C}_2 + \text{N} \leftrightarrow \text{CN} + \text{C}$. The necessity of considering the processes (3) remains also for the velocities 8 and 9 km/sec. For the velocity $V = 10 \text{ km/sec}$ the model of the main processes is extended owing to reactions with the participation of the electron e and charged particles CO^+ and C^+ (see below).

In the calculations of the radiation from atmospheric gases, of interest is not only its integral intensity but also its spectral composition. Under comparable conditions, the radiation of the air differs qualitatively from the radiation of the considered mixtures $\text{CO}_2\text{--N}_2\text{--Ar}$. We note two qualitative distinctions. First, for moderate velocities of flight the intensity of radiation from such mixtures is much higher than that of air and, second, in these mixtures the main radiation sources are molecules formed as a result of chemical reactions (CN, CO, C_2) [6] by analogy with nitrogen-oxide molecules in a high-temperature air. On the other hand, processes of electronic excitation of molecules that determine the entire radiation spectrum of the gas in the Mars atmosphere are not clearly understood, and the rate constants corresponding to them are determined with a large error (although, at the present time, there are works in which the above-mentioned cross sections were refined, for example, for CN and C_2 molecules [6]). In this connection, Table 1 presents the mechanisms (obtained for different shock-wave-front velocities V) of the main reactions that determine the distribution of the concentrations for CN, C_2 , and CO molecules without specifying the channels of their electronic excitation. Here and in Table 2 (see below), in the corresponding column of the chosen velocity V , a concrete structure of the main reaction and its direction necessary for modeling are specified. Table 1 also presents the

TABLE 1. Main Processes behind a Shock Wave Propagating in the Mars Atmosphere with Different Velocities of the Front V ($\varphi = n_{\text{CN}}, n_{\text{C}_2}, n_{\text{CO}}$; $\varepsilon = 0.3$; n_i is the concentration of particles)

Main reactions	log A	n	E_a	$V, \text{ km/sec}$						
				4	5	6; 7	8	9	10	11
$\text{CO}_2 + \text{M} = \text{CO} + \text{O} + \text{M}$	12.70	0.5	52310	→	→	→	→	→	↔	→
$\text{O} + \text{N}_2 = \text{N} + \text{NO}$	13.83	0	37980	→	→	→	↔	↔	→	
$\text{CO} + \text{N} = \text{CN} + \text{O}$	14.60	0	33080	↔	↔	↔	↔	↔	↔	↔
$\text{CO} + \text{C} = \text{C}_2 + \text{O}$	21.23	-1.5	57200	↔	↔	↔	↔	↔	↔	↔
$\text{CO} + \text{M} = \text{C} + \text{O} + \text{M}$	20.36	-1.0	129000	→	→	→	→	→	↔	→
$\text{N} + \text{O}_2 = \text{O} + \text{NO}$	9.81	1.0	3150	→	→	↔	↔	↔	↔	
$\text{O}_2 + \text{C} = \text{CO} + \text{O}$	12.97	0.25	0	→	→	→	→	→	→	
$\text{CO}_2 + \text{O} = \text{CO} + \text{O}_2$	13.22	0	27800	→	→	→	→	→	→	
$\text{CO}_2 + \text{N} = \text{NO} + \text{CO}$	11.93	0	1106	→	→					
$\text{O}_2 + \text{M} = 2\text{O} + \text{M}$	21.30	-1.5	59750				→	←		
$\text{NO} + \text{M} = \text{N} + \text{O} + \text{M}$	17.04	0	75500					→	→	
$\text{CN} + \text{O} = \text{NO} + \text{C}$	13.20	0.1	14600					↔	↔	
$\text{C}_2 + \text{N} = \text{CN} + \text{C}$	14.42	0	1400					↔	↔	↔
$\text{N}_2 + \text{C} = \text{CN} + \text{N}$	13.80	0	23200						→	
$\text{C}_2 + \text{M} = 2\text{C} + \text{M}$	14.57	0	69900							→
$\text{CN} + \text{CO}_2 = \text{NCO} + \text{CO}$	14.60	0	19200	→						
$\text{NCO} + \text{M} = \text{CO} + \text{N} + \text{M}$	16.80	-0.5	24080							→
$\text{C} + \text{O} = \text{CO}^+ + e$	8.944	1.0	33100						↔	↔
$\text{CO}^+ + \text{C} = \text{CO} + \text{C}^+$	10.97	0.67	6270						↔	↔
$\text{C} + e = \text{C}^+ + 2e$	33.59	-3.78	130700							↔

TABLE 2. Main Processes behind a Shock Wave Propagating in the Mars Atmosphere with Different Velocities of the Front V

Main reactions	$\varphi = n_e, \varepsilon = 0.5$						$\varphi = T, \varepsilon = 0.05$					
	$V, \text{ km/sec}$											
	5; 6	7	8	9	10	11	4; 5; 8	6	7	9	10	11
$\text{CO}_2 + \text{M} = \text{CO} + \text{O} + \text{M}$	→	→	→	→	→	→	→	→	→	→	→	→
$\text{O} + \text{N}_2 = \text{N} + \text{NO}$	→	→	↔	→	→	→				→	→	
$\text{CO}_2 + \text{O} = \text{CO} + \text{O}_2$	→	→	→					→				
$\text{N} + \text{O}_2 = \text{O} + \text{NO}$	→	↔	↔	↔								
$\text{O}_2 + \text{M} = 2\text{O} + \text{M}$			←						↔	←	←	
$\text{O}_2 + \text{C} = \text{CO} + \text{O}$			→								→	
$\text{NO} + \text{M} = \text{N} + \text{O} + \text{M}$			→	→	→	→				→	→	
$\text{CO} + \text{N} = \text{CN} + \text{O}$				↔	↔	↔				↔	↔	
$\text{CN} + \text{O} = \text{NO} + \text{C}$				↔	↔	↔				↔	↔	
$\text{N}_2 + \text{C} = \text{CN} + \text{N}$					→	→						
$\text{CO} + \text{M} = \text{C} + \text{O} + \text{M}$					→	→					→	→
$\text{N} + \text{O} = \text{NO}^+ + e$	↔	↔	↔	↔								
$\text{O} + \text{O} = \text{O}_2^+ + e$	↔	↔	↔	↔								
$\text{C} + \text{O} = \text{CO}^+ + e$				↔	↔	↔						↔
$\text{CO}^+ + \text{C} = \text{CO} + \text{C}^+$				↔	↔	↔						↔
$\text{C} + e = \text{C}^+ + 2e$					↔	↔						↔

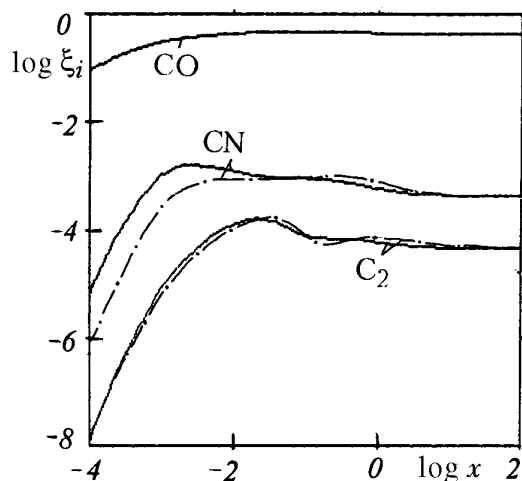


Fig. 3. Distribution of the molar fractions ξ_i for CO_2 , CN, and C_2 molecules versus distance x (cm) from the shock-wave front. The solid lines denote the data calculated with the use of the initial data base containing the data on 124 reactions, the dash-dot lines denote the data calculated with the use of the model containing 12 main reactions for $V = 9$ km/sec (see Table 1). $P_1 = 133.3$ Pa, 96% of $\text{CO}_2 + 3\%$ of $\text{N}_2 + 1\%$ of Ar.

parameters of the rate constant of the direct reaction in the form of the generalized Arrhenius formula $k_j = AT^n \exp(-E_a/RT)$. For the reactions given in the table, the rate constants have the dimensions of $\text{cm}^3/(\text{mole}\cdot\text{sec})$, and the activation energy E_a has the dimensions of K. In Table 1, the data on the rate constants with the participation of M are given for $M = \text{CO}_2$. The relative efficiency of the remaining particles is given in [5]. In this case, we, naturally, assume that excitation and deactivation channels of type (3) can be included in the mechanisms presented in Table 1 if reliable data on the rate constants k_j of these processes are at hand. Even though the electronically excited particles make the main contribution to the radiation spectrum of the Mars atmosphere, they are very small components whose concentrations are much lower than the concentrations of the components in the ground states. Because of this, the influence of the errors of determining the rate constants k_j of formation of these particles in electronic states on the distribution of the total concentrations of CN, C_2 , and CO components (without specifying the degree of electronic excitation) is practically absent.

Figure 3 presents the distributions of the concentrations of CO, CN, and C_2 behind the shock-wave front, obtained using the initial data base and a small mechanism of the main reactions for $V = 9$ km/sec.

For the problems of heat exchange and radio communication with a spacecraft, of importance is the determination of the gas temperature and the concentration of charged particles. As a quantitative characteristic of the total concentration of charged particles, the electron density n_e can be chosen. Table 2 presents the mechanisms of the main kinetic processes, in which the translational temperature of the gas ($\varphi = T$, $\varepsilon = 0.05$) and the concentration of the electrons ($\varphi = n_e$, $\varepsilon = 0.5$) are used as the investigated functional. Just as in Table 1, the mechanisms presented in Table 2 correspond to different velocities of the shock-wave front V .

We note some features of the results obtained. When $\varphi = T$, the set of the main physicochemical processes includes a minimum number of reactions (for example, it is a subset of the model for $\varphi = n_e$), and the complete set of the main reactions (from Table 1) which determine the distribution of the concentrations of CN, C_2 , and CO corresponds to both the mechanism by the electron e and the mechanism by the temperature T . Immediately behind the shock-wave front, CO_2 molecules dissociate and the reaction $\text{CO}_2 + M \rightarrow \text{CO} + \text{O} + M$ appears in all the mechanisms obtained. N_2 molecules decay not as a result of dissociation, but as a result of the exchange reaction $\text{N}_2 + \text{O} \rightarrow \text{NO} + \text{O}$. In the case where the front velocity is $V \leq 8$ km/sec,

electrons form predominantly in the course of the associative-recombination reactions $N + O \leftrightarrow NO^+ + e$ and $O + O \leftrightarrow O_2^+ + e$ (not shown in Table 1), while at velocities of ≈ 9 km the mechanism changes and for $V \geq 10$ km/sec, electrons and ions form predominantly in the reactions $C + O = CO^+ + e$, $C + e = C^+ + 2e$, and $CO^+ + C = CO + C^+$. We note that in the Mars atmosphere, the translational temperature T behind the front of a shock wave propagating with velocities $V \leq 8$ km/sec (and accuracy $\varepsilon = 0.05$) is determined by only 1–2 processes. The model should be extended in the case where $V \geq 9$ km/sec.

Thus, the results presented show that the initial base of physicochemical data describing the non-equilibrium processes occurring behind a shock wave in the Mars and Venus atmosphere can be significantly simplified. As a result, we are able to choose a small number of the main physicochemical processes, the use of which in numerical modeling will allow us to describe adequately such important characteristics as the distribution, the electron concentration, radiation, and the gas temperature.

This work was carried out with financial support from the International Science and Technology Center, project 1549–00.

NOTATION

T , T_v , and T_e , translational, vibrational, and electronic temperatures, respectively; ϕ , investigated functional; ε , threshold accuracy; n_e , concentration of electrons; n_i , concentration of the components ($i = CN, C_2, CO$); ξ_i , molar fraction of the i th component; k_j , rate constant of the j th process; $k(T, T_v)$, two-temperature constant of the reaction rate; $k^0(T)$, thermally equilibrium rate constant; $Z(T, T_v)$, nonequilibrium factor; P_1 , pressure ahead of the shock-wave front; V , shock-wave velocity; x , distance from the shock-wave front; L_f , mean-free path behind the shock-wave front; A , n , and E_a , parameters of the rate constant of a reaction.

REFERENCES

1. V. N. Makarov, *Kvantovaya Élektron.*, **24**, No. 10, 895–899 (1997).
2. V. N. Makarov, *Khim. Fiz.*, **18**, No. 4, 48–52 (1999).
3. C. Park, J. T. Howe, R. L. Jaffe, and G. V. Candler, *J. Thermophys. Heat Trans.*, **8**, No. 1, 9–23 (1994).
4. J. S. Evans, C. J. Schexnayder, and W. L. Grose, *J. Spacecraft Rockets*, **11**, No. 2, 84–88 (1974).
5. R. N. Gupta and K. P. Lee, *An Aerothermal Study of MESUR Pathfinder Aeroshell*, AIAA Paper 94–2025 (1994).
6. G. N. Zalogin, P. V. Kozlov, L. A. Kuznetsova, et al., *Radiation in a CO₂–N₂–Ar Mixture in Shock Waves: Experiment and Theory*, Preprint No. 40–98, Institute of Mechanics, Moscow State University [in Russian], Moscow (1998).
7. G. N. Zalogin, V. V. Lunev, and Yu. A. Plastinin, *Izv. Akad. Nauk SSSR, Mekh. Zhidk. Gaza*, No. 1, 105–112 (1980).
8. G. N. Zalogin, *Izv. Akad. Nauk SSSR, Mekh. Zhidk. Gaza*, No. 6, 81–87 (1974).
9. V. N. Makarov, *Prikl. Mekh. Tekh. Fiz.*, **37**, No. 2, 69–82 (1996).
10. L. V. Gurvich and N. P. Rtishcheva, *Teplofiz. Vys. Temp.*, **3**, No. 1, 33–46 (1965).
11. E. A. Kovach, S. A. Losev, and A. L. Sergievskaya, *Khim. Fiz.*, **14**, No. 9, 44–76 (1995).
12. G. G. Chernyi and S. A. Losev (eds.), *Physicochemical Processes in Gas Dynamics: Computerized Reference Book in Three Volumes*, Vol. 1: *Dynamics of Physicochemical Processes in a Gas and a Plasma* [in Russian], Moscow (1995).